RSC Advances

ROYAL SOCIETY OF CHEMISTRY

www.rsc.org/advances

TOC GRAPHICS

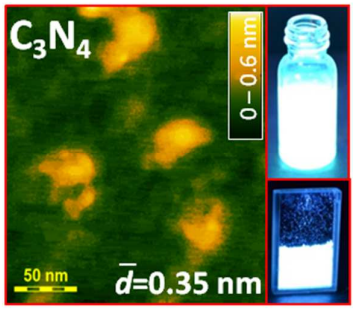

Cite this: DOI: 10.1039/c0xx00000x

www.rsc.org/xxxxxx

ARTICLE TYPE

Preparation and optical properties of highly luminescent colloidal single-layer carbon nitride

Yaroslav V. Panasiuk[a], Alexandra E. Raevskaya[a], Oleksandr L. Stroyuk*[a], Petro M. Lytvyn[b], Stepan Ya. Kuchmiy[a]

Received (in XXX, XXX) Xth XXXXXXXXX 20XX, Accepted Xth XXXXXXXXX 20XX
DOI: 10.1039/b000000x

Thermal treatment of graphitic carbon nitride (g-CN) in aqueous solutions of tetraethyl ammonium hydroxide at ~100 °C yields transparent colloidal solutions retaining stability at the CN concentration of up to 50 g/L and upon dilution by a factor of 10^3. Atomic force microscopy showed that the major part of the CN particles in diluted colloidal solutions are characterized by a lateral size of around 30–50 nm and a thickness of 0.3–0.4 nm typical for the single CN layer. Besides, a small fraction of multi-layer 2–5-nm-thick g-CN particles with a size of ~ 60 nm is present in the solutions. Photoexcitation of the colloidal CN near the edge of the absorption band results in emission of strong broad-band photoluminescence with a maximum at 460–470 nm and a quantum yield of 45–50%.

Introduction

Explosive growth of interest in graphene and graphene-based materials resulted in a variety of new methods of graphite exfoliation[1–4] and inspired interest to other layered compounds such as MoS_2 and WS_2[5], as well as graphitic carbon nitride (g-CN)[6–11]. The g-CN exhibits catalytic and photocatalytic properties in a broad range of redox-processes[6–11]. High photocatalytic activity of the g-CN coupled with the visible-light sensitivity, chemical and photochemical stability, and the doping-dependent electronic properties[8,11–15] were the reasons to praise the g-CN as "a rising star of photocatalysis"[11]. Following the layered chalcogenides one can expect that exfoliation of the bulk g-CN to single layers will strongly affect the photophysical and photochemical properties of carbon nitride. Truly to this expectation, it was found that single-layer CN and a-few-layer g-CN are much efficient photocatalysts of water reduction[16,17] and ammonia oxidation[18], as compared to the bulk g-C_3N_4. The advanced photocatalytic[16–19] and photoelectrochemical[17,21,22] activity of the exfoliated g-CN was attributed to a longer life span of the photogenerated charge carriers[19] and favourable conditions for charge migration along the basal plane of the single CN layers[23].

At the same time, only a few methods were reported on the synthesis of single-layer CN and a-few-layer g-CN. The bulk g-C_3N_4 can be converted into a-few-layer CN nanosheets by ultrasound (US) treatment[20,23]. Prolonged (16 h) sonication of the bulk g-CN in water followed by centrifugation at 15000 rpm allowed to produce colloidal CN nanosheets with a yield of around 9%[24]. Similar method was employed to produce 2–3-nm thick CN nanoflakes in water[25]. Thinner (around 1 nm thick) CN nanosheets can be produced by 8-h sonication in ethanol[26]. Dispersions of 2-nm-thick CN nanosheets can be synthesized by the US treatment also in 2-propanol, N-methylpyrrolidone and acetone[27].

The US-assisted exfoliation of the bulk g-CN is accelerated by preliminary intercalation or partial oxidation of g-CN similarly to the graphite[2–4]. For example, the US exfoliation of the bulk g-CN can be achieved after intercalation of lithium atoms from Li solution in ammonia[16]. The single-layer CN can also be produced via intercalation of the bulk carbon nitride with H_2SO_4 followed by US treatment[21,28]. The US-assisted exfoliation of the product of partial oxidation of the bulk g-CN with HNO_3 yields a-few-layer 70–100-nm g-C_3N_4 particles with a thickness of ~5 nm[29]. The strongly luminescent single-layer CN can be produced by a quite elaborate method[23] including the seasoning of the bulk g-CN in a mixture of concentrated nitric and sulphuric acids followed by the hydrothermal treatment of partially oxidized g-CN in concentrated aqueous ammonia solution and the US-assisted exfoliation in water.

An alternative route to the exfoliated g-CN is based on the pyrolysis of CN precursors (dicyandiamide, melamine, etc.) in combination with compounds producing copious amounts of gaseous pyrolysis products. Permeation of the gases between the layers of forming g-CN allows to produce a-few-layer g-C_3N_4 particles by a one-step synthesis. For example, simultaneous pyrolysis of melamine and $NaBH_4$ yields 1.5-nm-thick g-CN particles[30]. The thermal decomposition of a mixture of dicyandiamide with NH_4Cl results in formation of a-few-layer g-CN particles with a thickness of around 2 nm[17].

It should be noted that feasibility of the direct exfoliation of the bulk g-CN to single layers in liquid dispersive media similar to the exfoliation of graphite in pyrrolidone derivatives or polyhalogenated benzenes[2,5] has not yet been reported.

Recently we have shown that the bulk g-CN produced by the urea pyrolysis can be dispersed in aqueous tetraethyl ammonium hydroxide (NEt_4OH) solutions at 98–100 °C[31]. However, the thickness of the g-CN particles in the produced colloidal

solutions, 6–8 nm, was much larger than the thickness of the single layer carbon nitride, ~0.4 nm[19,21–23,28]. We have assumed that by varying conditions of the exfoliation of bulk g-CN in NEt_4OH solutions, in particular, the nature of molecular precursor used to synthesize the bulk g-C_3N_4 as well as the pyrolysis conditions, the exfoliation process can be directed preferably to the route of formation of the single-layer CN particles.

In the present paper we show that thermal treatment of the bulk g-CN, produced from melamine (1,3,5-triaminotriazine) in air at 650 °C, in aqueous NEt_4OH solutions at ~100 °C results in the g-CN exfoliation to the single-layer carbon nitride particles with a thickness of 0.35 nm emitting strong photoluminescence in the visible spectral range.

Experimental methods

To produce bulk g-CN melamine was placed into open quartz vessel and annealed in air in an oven at 650 °C for 2 h (please refer to Electronic Supplementary Information (ESI) for a more detailed description of the choice of the pyrolysis conditions). The oven temperature was elevated from 25 °C to 650 °C with a rate of ~15° per min. The mass yield of the product was 15–16%. The g-CN was cooled to room temperature, grinded in a mortar and stored at ambient conditions in the dark.

Colloidal CN was produced by dispersion of the bulk carbon nitride in aqueous solution of NEt_4OH (1.36 M) at ~100 °C. In a typical procedure, 1.0 g g-CN was mixed with 20 mL aqueous NEt_4OH solution and kept for 4 h at boiling temperature with magnetic stirring and using a reflux condenser to avoid solvent evaporation. The bulk g-CN was completely dissolved giving the mass concentration of 50 $g \times L^{-1}$ and a molar C_3N_4 unit concentration of 0.54 M. The solution is optically transparent and retains stability toward aggregation and formation of a sediment for many months. After centrifugation at 3000 rpm the sediment forms with a mass smaller than 4–5% of the original mass of bulk g-CN dissolved in NEt_4OH solution. At a higher g-CN content the complete dissolution cannot be achieved.

To prepare samples for Fourier transform infrared (FTIR) spectroscopy and atomic force microscopy (AFM) the original concentrated CN solution was subjected to the dialysis against distilled water for 24 h using CelluSep H1 1 KDa membranes (Orange Scientific).

The hydrodynamic size of colloidal CN particles was determined by the dynamic light scattering (DLS) spectroscopy on a Malvern ZetaSizer Nano S at 22 °C. FTIR spectra were recorded on a Perkin Elmer Spectrum One spectrometer. To obtain FTIR spectra the samples (0.1 g of melamine, the bulk g-CN, a residue produced by solvent evaporation from purified CN colloid) were mixed with 0.1 g KBr and pressed into pellets at 10 MPa. Experiments on nuclear magnetic resonance (NMR) on ^{13}C nuclei were performed on a Bruker DRX 500 Avance spectrometer. The samples for NMR were prepared by mixing the CN colloid with D_2O in a volume ratio of 1:5. AFM data were collected with a NanoScope IIIa Dimension 3000^{TM} scanning probe microscope. The height and phase-contrast images were taken simultaneously over the same areas. The ultra sharp silicon tips were used to improve the lateral resolution. The samples were prepared by dropping colloidal CN solution onto the surface of freshly slivered mica plate followed by drying in the hot air flow. Original concentrated CN colloid was diluted in 1000 times to produce samples for AFM. After drying the sample was rinsed one time with 1% aqueous solution of acetic acid and several times with distilled water.

The elemental (C, H, N) analysis was performed on a CHN Analyzer Mod. 1106 (Carlo Erba) by a modified Pregl-Dumas method via burning of the sample (1.0 mg) in oxygen flow over Cr(III) oxide at ~1030 °C, followed by reduction of nitrogen oxide and O_2 over a copper grid at 650 °C and chromatographic analysis of N_2, CO_2 and H_2O.

Absorption and diffuse reflectance spectra were registered using a Specord 210 and a Shimadzu UV-3600 spectrophotometers, respectively. Photoluminescence (PL) and PL excitation spectra were recorded on a Perkin-Elmer LS 55 spectrometer. The PL quantum yield Φ was determined using solid extra pure anthracene (Fluka) as a reference standard (Φ_{ref} = 100%). The powder samples were placed in standard quartz capsules and studied in a standard LS 55 accessory for powdered samples. The solutions were studied in the same accessory in 1.0-mm quartz cuvettes. The light absorption by solutions was complete as the optical density of the samples at the excitation wavelength exceeded 2–2.5. In this way, PL was emitted only from a thin surface layer irrespectively of the sample state and collected at an angle of 90° with respect to the exciting light beam. Identical measurement conditions (cuvette, slits, spectrum registration rate, etc.) were maintained for the reference and work samples. The PL quantum yield of work samples was calculated as $\Phi_w = (I_w/I_{ref}) \times \Phi_{ref}$, where I_w and I_{ref} is the integral PL intensity of the work sample and reference, respectively.

Results and Discussion

Characterization of bulk g-C_3N_4. Calcination of melamine at 650 °C in air yields beige-colour graphitic carbon nitride powder with a mass yield of 15–16%. The X-ray diffraction pattern of the bulk g-C_3N_4 (ESI, Fig. S1) reveals a peak at 2θ = 27.8° corresponding to the distance between CN layers d_{002} = 0.321 nm. The d value fits to the range reported for the g-CN – from 0.319 nm to 0.326 nm[17,21–23,30]. Additionally, a low-intensity peak at ~13° can be observed that corresponds to an in-plane periodicity of heptazine building blocks in CN layers, 0.68 nm[17,21–23,30].

The elemental analysis of the bulk carbon nitride showed that it is composed of 61 w.% nitrogen, 38 w.% carbon and ~1 w.% hydrogen. The C and N content corresponds closely to stoichiometric C_3N_4 (61 w.% N and 39 w.% C). The hydrogen atoms originate, most probably, from the amino-groups of g-CN.

The FTIR spectrum of the bulk g-CN (Fig. 1, curve 2) contains a band at 810 cm^{-1} – the so-called "fingerprint" of the triazine and heptazine heterocycles as well as an additional series of characteristic bands in the range of 1200–1660 cm^{-1} originating from the vibrations of N–C=N fragments of the heptazine heterocycles[17,20–23].

Some differences between the IR spectra of melamine and the bulk g-CN (Fig. 1, curves 1 and 2) can be distinguished. In particular, the melamine condensation into g-C_3N_4 results in an increase of the number of the characteristic bands at 1150–1300 cm^{-1} indicating expansion of the conjugated heterocyclic system

and an increase in the number of allowed deformational vibrations[32].

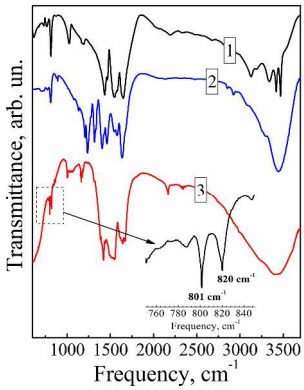

Fig. 1 FTIR spectra of melamine (curve 1), bulk g-C_3N_4 (2), and exfoliated CN (3).

Besides, the condensation is followed by extinction of the band at 2200 cm^{-1} typical for a combined vibration of N–H and C=N bonds in melamine[33,34] as well as vanishing of the fine structure of the band at 3000–3700 cm^{-1} corresponding to the valence vibrations of N–H bonds in amino-groups and O–H bonds in adsorbed water.

Characterization of colloidal carbon nitride. Thermal treatment of the bulk g-C_3N_4 in boiling aqueous NEt_4OH solution results in gradual dissolution of the g-CN powder and formation of stable colloidal solutions showing no apparent signs of the light scattering. After complete g-CN dispersion and cooling to room temperature the solutions retain long-term stability to aggregation at quite a high CN content – up to 50 g/L corresponding to a molar concentration of 0.54 M in terms of C_3N_4 units. Optical transparency of the solution indicates that the size of individual CN particles is of an order of 100 nm and smaller.

Similar treatment of the g-CN powder in aqueous NaOH solution yields opaque and unstable suspensions. No dissolution of the bulk g-CN is also observed in aqueous NEt_4Br solution containing solely tetraethyl ammonium cation as well as in NH_4OH solution. Therefore, the presence of NEt_4OH is a prerequisite for dissolution of the bulk g-CN and formation of stable and transparent colloids.

Dynamic light scattering spectroscopy shows that the average hydrodynamic size *L* of colloidal particles in as-prepared concentrated solutions is around 800 nm (Fig. 2, curve 1). As the light scattering can not be observed by the naked eye we assumed that the particles are formed by loose association of much smaller structural units, most probably via hydrogen bond formation. The assumption is supported by DLS spectroscopy showing that *L* depends on the concentration of colloidal carbon nitride. Dilution of the original colloid by 10 times results in a decrease of the hydrodynamic size of colloidal particles to ~200 nm (Fig. 2, curve 2). Further dilution in 100 and 1000 times (with respect to original concentrated colloid) is accompanied by a decrease of *L* to ~100 nm and ~50 nm, respectively (Fig. 2, curves 3 and 4). No further changes of *L* were observed at a higher dilution factor indicating that the average hydrodynamic size of structural units participating in formation of large associates in the concentrated solution is around 50 nm.

Figure 3 shows a height-contrast AFM image of particles present in the CN colloid (1000-times dilution). Two fractions of particles can be distinguished on the AFM images – a fraction of the nanoplates with a lateral size of around 60 and a thickness higher than 1 nm and a fraction of smaller particles with a thickness lower than 1 nm. The height profiles on Fig. 3 show that the thickness of the particles of the first sort is 2.0–4.5 nm.

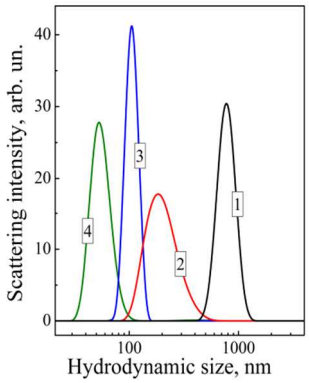

Fig. 2 Hydrodynamic size distribution of colloidal CN particles in original concentrated solution (curve 1) and after dilution by a factor of 10 (2), 100 (3), and 1000 (4). $[C_3N_4] = 5.4\times10^{-1}$ M (curve 1), 5.4×10^{-2} M (2), 5.4×10^{-3} M (3), 5.4×10^{-4} M (4).

As the single layer CN is 0.323 nm thick[19, 21–23], we conclude that such particles are multi-layered and composed of 5–15 single layers of carbon nitride. It should be noted that the number of smaller particles thinner than 1 nm is much higher than the number of larger multi-layered nanoplates. Figure 4a shows AFM image taken at a higher magnification where several particles thinner than 1 nm can be observed. In such thickness range some of the bright contrast areas (hillocks) in the height map can represent artefacts originating not from the CN particles but from rougher areas of the mica substrate.

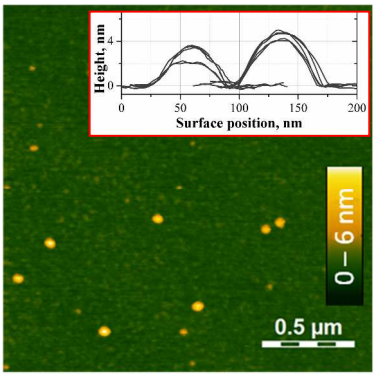

Fig. 3 AFM image of colloidal CN particles. Insert: height profiles of several CN particles thicker than 1 nm.

To distinguish between the real CN particles and artefacts phase-contrast AFM images were simultaneously recorded in the same areas of sample. Figure 4b and additional AFM images of a lower magnification given in ESI (Fig. S2, S3) show that some of the bright contrast areas observed in the AFM height map indeed originate from irregularities of the mica surface. Nevertheless, the phase-contrast data clearly separate CN particles and mica irregularities due to difference in their visco-elastic properties and

a weak coupling between the CN particles and the substrate.

Analysis of the height profiles for the CN particles (Fig. 4c) showed that such particles have an average thickness of 0.35 nm corresponding well to the reported thickness of the single layer carbon nitride[19,21–23,28]. The single-layer CN particles are characterized by an average lateral size of 43 nm with a standard deviation of ±8 nm (ESI, Fig. S3). The result is in good accordance with the DLS data on the average hydrodynamic size of CN particles in the colloidal solution used to prepare the sample for AFM. Summarizing the discussion of the AFM results we can, therefore, conclude that the CN colloid after 1000-times dilution contains predominantly single-layer CN flakes with an average thickness near 0.35 nm and a mean lateral size of 43 nm. A low-population fraction of the multi-layer g-CN particles with a thickness of 3–5 nm and a lateral size of around 60 nm is also present in the solution. No peak corresponding to such particles can be found in the DLS spectrum of the colloid (Fig. 2, curve 4) corroborating the conclusion on a scarce population of such particles.

The FTIR spectrum of colloidal CN particles (Fig. 1, curve 3) differs somewhat from the IR spectrum of the bulk g-C_3N_4 (curve 2) and resembles rather the IR spectrum of melamine (curve 1). Exfoliation of the bulk g-CN is accompanied with extinction of some of the N–C=N vibration bands at 1150–1300 cm^{-1} indicating rupture of the extensive system of conjugated heptazine heterocycles of the bulk g-CN and formation of much smaller particles[32]. The combined N–H and C=N vibration band at ~2200 cm^{-1} becomes visible again attesting to the presence of a large number of amino-groups in the colloidal CN particles[33,34]. The bands at 980–1220 cm^{-1} can be assigned to the C–N bond vibrations in the NEt_4^+ cation. Additionally, two weak bands can be distinguished at 1162 cm^{-1} and 1315 cm^{-1} (ESI, Fig. S4, curve 3), that are absent in the IR spectra of melamine (Fig. 1, curve 1), bulk g-CN (ESI, Fig. S4, curve 1) and pure NEt_4OH (Fig. S4, curve 2). The bands can be assigned to the C–O valence vibration and COH deformation vibration of tertial alcohol/phenolic hydroxyl group[35], respectively. The fact indicates presence of a small amount of C–OH groups in the dispersed CN formed as a result of partial hydrolysis of the $N(C)_3$ (C–NH–C) bridge groups in the CN particles during exfoliation. Ionization of C–OH groups in the basic NEt_4OH medium and electrostatic repulsion between the CN particles can contribute to stabilization of carbon nitride colloids. The assumption is corroborated by the fact of fast precipitation of the colloid after neutralization of NEt_4OH by acetic acid. Also, the Z-potential of colloidal CN particles was found to be negative and small, around -8 – -9 mV at neutral pH.

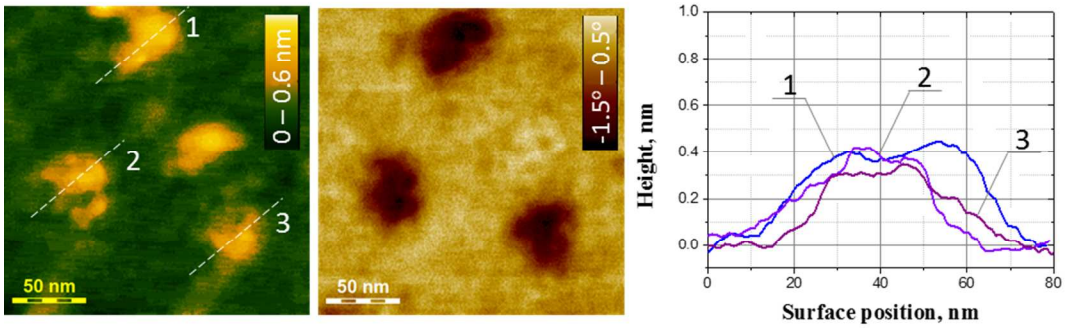

a b c

Fig. 4 AFM height map (a) and corresponding phase contrast image (b) of CN particles on mica. Height profile of CN particles (c) measured along lines marked on (a).

It should be noted that the "fingerprint" band of triazine/heptazine heterocycles at 810 cm^{-1}, typical for the bulk g-CN, splits into two bands with maxima at 801 and 820 cm^{-1} upon exfoliation and formation of single-layer CN particles. Such splitting indicates the presence of at least two different heptazine-based moieties in the system under study. For example, similar splitting was observed in the IR spectrum of a melem-melam adduct, where the components were associated by the hydrogen bonds[32]. Splitting of the "fingerprint" band was also observed for binary adducts of triazine derivatives[33] as well as for molecules comprising two heptazine fragments in a different environment[36]. The IR spectroscopy results in combination with the AFM data indicate, therefore, that the CN colloid contains at least two major components – the single-layer CN particles and smaller heptazine-based fragments that most probably originate from partial hydrolysis of CN sheets during the exfoliation.

The NMR ^{13}C spectrum of colloidal CN particles (ESI, Fig. S5) shows two strong signals at 6 and 52 ppm belonging to ethyl groups of the NEt_4^+ cations and a group of signals in the range of 156–171 ppm indicating the presence of a mixture of heptazine-based species in colloidal solution. Two principal signals of the group, 157 and 167.5 ppm, can be assigned to the internal C (CN_3) and external C (N_2CNH_2) atoms in melon/carbon nitride[32,37–39]. The medium intensity signals at 169–171 ppm and weak signals at 162 ppm and around 168 ppm are close to the signals reported for $C_6H_7O^-M^+$ (M – alkali metals) produced by basic hydrolysis of melem[38]. Finally, two medium intensity signals near 166 ppm resemble those reported for the N_2CNH_2 fragments in melem[38]. The two latter groups of signals can be assigned to the products of partial hydrolysis of CN particles resulting in formation of smaller species bearing simultaneously COH and CNH_2 groups.

It should be noted that an accurate elemental analysis of colloidal CN after dialysis and solvent evaporation is hindered by occlusion of NEt_4OH as evidenced by the FTIR spectroscopy, its amount depending on the evaporation conditions. Obviously, the partial hydrolysis of CN particles in the course of the dispersion results in some deviation from the C_3N_4 stoichiometry. At the same time,

the FTIR and NMR results show the amount of hydrolysis products to be rather low, and, therefore, this deviation is expected to be small. In this view, a C_3N_4 molar unit was adopted as an approximation to express molar concentration of colloidal CN and to calculate extinction coefficients of the single-layer CN particles as discussed below.

Spectral properties and photoluminescence of colloidal CN. Absorption spectrum of concentrated (0.54 M C_3N_4) CN colloid (Fig. 5a, curve 1) reveals a band with an edge at ~460 nm, a distinct peak at ~395 nm and a low-intensity "shoulder" at 415–430 nm. The molar extinction coefficient (calculated in terms of a C_3N_4 unit) in the band maximum is quite small, $\varepsilon_{395} = 3\ M^{-1}\times cm^{-1}$. The low ε value allows us to attribute the absorption band to a $n\pi^*$-transition[40] with the participation of free electron pairs of nitrogen atoms in heptazine heterocycles and amino-groups of the colloidal CN. Identification of the $n\pi$-type of the band via blocking the transition by protonation of N atoms is hindered by the coagulation of the concentrated colloid in the presence of acids.

Dilution of the original concentrated colloid reveals additional shorter-wavelength components in the absorption spectrum of CN particles. In particular, a low-intensity shoulder at 325–345 nm can be distinguished in the spectrum after the 10-times dilution (Fig. 5b, curve 1a) with a molar extinction coefficient of 12–13 $M^{-1}\times cm^{-1}$ at 330 nm. After the 1000-times dilution of the concentrated CN colloid a shoulder at 275–300 nm (ε_{290} = 1070 $M^{-1}\times cm^{-1}$) and a peak at 245–250 nm (ε_{250} = 5330 $M^{-1}\times cm^{-1}$) are observed (Fig. 5b, curve 1b). These spectral features can also be attributed to the $n\pi^*$-type transitions by values of the molar extinction coefficients[40]. The assignment is supported by a considerable quenching of the latter two bands upon addition of acetic acid (compare curves 1b and 1c). It should be noted that the colloidal CN retains stability at low pH after 1000-times dilution, contrary to the concentrated colloid. Finally, after the 10000-times dilution an intense band with a maximum at 205–207 nm (ε_{206} = 24600 $M^{-1}\times cm^{-1}$) becomes clearly visible (curve 1d). The high molar extinction coefficient and spectral position of the band as well as its insensitivity to pH justify attribution of the band to a $\pi\pi^*$-transition in the aromatic heptazine fragments of the CN particles[40].

Photoexcitation of the concentrated colloidal CN at λ_{ex} = 415 nm results in emission of intense photoluminescence (PL) in a broad band (Fig. 5a, curve 2) with a maximum at 460–470 nm (2.65–2.70 eV) and a spectral width of 65 nm (0.36 eV). The emission colour of CN particles can be characterized as "cold" white (see photo 2 in Fig. 5c). Estimations made using the solid anthracene as a reference showed that the PL quantum yield of the single-layer CN is as high as 45–50%. The high emission intensity opens opportunities of application of the single-layer carbon nitride as a LED emitter and a component of various photoluminescent materials and bio-labels.

The PL excitation spectrum of the concentrated colloidal CN (Fig. 5a, curve 3) registered in the PL band maximum (at λ_{PL} = 470 nm) shows two peaks at 405 and 420 nm corresponding well to the peak and the shoulder in absorption spectrum. The accordance between the absorption and PL excitation spectra of colloidal CN confirms that the photoexcited CN is the source of PL emitted in the visible spectral range. The emission, similar by the spectral parameters and a quantum yield of ~10%, is observed also for the bulk g-CN.

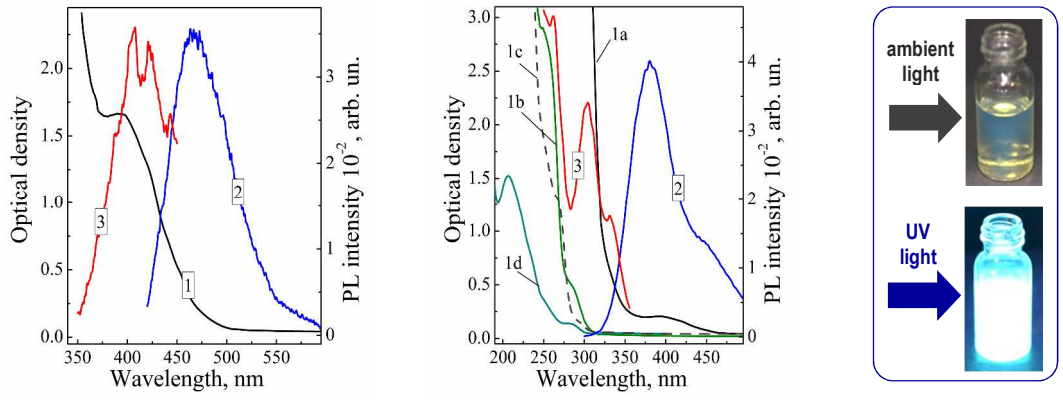

Fig. 5 (a,b) Absorption (curves 1), photoluminescence (curves 2) and PL excitation (curves 3) spectra of concentrated (a) and diluted (b) colloidal CN. In (b): curves 1a–1d correspond to CN colloid diluted in 10 (1a), 1000 (1b), 10000 times (1d), curve 1c – 0.01 M CH_3COOH added to 1b. PL is excited by λ_{ex} = 395 nm (a) and λ_{ex} = 290 nm (b); (c) Photographs of CN colloid under illumination with ambient solar light and under 350–370-nm UV light.

The PL spectrum of colloidal CN recorded at excitation with λ_{ex} = 260 nm, i.e. into the absorption shoulder of the colloidal solution diluted by 1000 times ([C_3N_4] = 5.4×10^{-4} M, Fig. 5b, curve 1b), differs drastically from the PL spectrum of the original concentrated colloid excited by λ_{ex} = 415 nm (compare curves 2 in Fig. 5a and 5b). At excitation with λ_{ex} = 260 nm a new band with a maximum at 390 nm appears in the PL spectrum of the colloidal CN. At that, the visible PL band centred at 465–470 nm is discernible only as a low-intensity shoulder. The PL emission from a higher (second, third, etc.) excited state of the CN particles is hardly probable according to the Kasha rule[40]. Therefore, the presence of at least two emitting species in the colloidal CN solution should be assumed, the first one responsible for the longer-wavelength PL band with a maximum at 465–470 nm and the second one generating the UV PL band with a maximum at 390 nm. At excitation of the colloidal particles with λ_{ex} = 260 nm both luminophors are excited simultaneously and contribute to the PL spectrum according to

their molar extinction coefficients on the excitation wavelength. The quantum yield of PL emitted in the band centred at 390 nm, ~5%, is much lower than the yield of the visible PL indicating a broader variety of radiationless relaxation routes for the species responsible for the UV PL band.

In the range of $\lambda < 350$ nm the PL excitation spectrum of the colloidal CN reveals a series of peaks at 260, 300 and 330 nm (Fig. 5b, curve 3) that mimic in general the positions of the absorption spectrum features observed at a various dilution grade (Fig. 5b, curves 1a,b). Moreover, the PL excitation spectra registered at 460 and 390 nm are almost identical. In the light of the above-discussed arguments in favour of the presence of at least two types of luminescing species in the system under study one should therefore assume that the luminophors have very similar structures and similar absorption bands in the range of $\lambda <$ 350 nm. The most probable candidates on the role of UV emitting luminophor is the above-discussed products of partial hydrolysis of CN sheets revealed by FTIR and ^{13}C NMR spectroscopy as well as their adducts with CN particles.

Conclusions

Thermal treatment of the bulk graphitic carbon nitride in aqueous solutions of tetraethyl ammonium hydroxide at ~100 °C results in dissolution of the g-CN and formation of stable and transparent colloidal solutions retaining stability at CN concentration of up to 50 g/L. The average hydrodynamic size of CN particles is around 0.8 μm and decreases to ~50 nm after the 1000-fold dilution indicating associated character of the CN particles in the original concentrated colloid.

Atomic force microscopy data showed that a dominant fraction of colloidal CN particles in diluted solutions is characterized by a lateral size of 30–50 nm and an average thickness of 0.35 nm typical for the single layer carbon nitride. Besides, a low-population fraction of larger multi-layered carbon nitride nanosheets with a size of around 60 nm and a thickness of 2–5 nm is present in colloidal solutions. The results of FTIR and ^{13}C NMR spectroscopy suggest that partial hydrolysis of CN sheets takes place during the exfoliation. The products of hydrolysis form adducts with CN sheets manifesting by a splitting of characteristic heptazine IR band at ~810 cm^{-1}.

The colloidal carbon nitride exhibits absorption band with an edge at ~460 nm. Photoexcitation into this band results in emission of the broad-band photoluminescence with a band maximum at 460–470 nm and a quantum yield of 45–50%. When excited by UV light with $\lambda = 260$ nm the colloidal CN exhibits second PL band with a maximum at 390 nm and a quantum yield of 5% which can be attributed to emission of the products of partial hydrolysis of carbon nitride and their adducts with CN particles.

Acknowledgements

The authors acknowledge the help of Dr. O.V. Svets (L.V. Pysarzhevsky Institute of Physical Chemistry of NASU) in acquiring the FTIR and XRD data.

Notes and references

[a] *L.V. Pysarzhevsky Institute of Physical Chemistry of National Academy of Sciences of Ukraine, 31 Nauky prosp., 03028, Kyiv, Ukraine, Fax: +380 44 525 0270; Tel.: +380 44 525 0270; E-mail: alstroyuk@ukr.net*
[b] *V.E. Lashkaryov Institute of Semiconductor Physics of National Academy of Sciences of Ukraine, 41 Nauky prosp., 03028, Kyiv, Ukraine, Fax: +380 44 525 5940; Tel.: +380 44 525 5940, E-mail: plyt@isp.kiev.ua*
The authors declare no competing financial interests.

† Electronic Supplementary Information (ESI) available: [ESI contains details of the g-CN synthesis, XRD pattern of bulk g-C_3N_4, phase-contrast AFM images of the single-layer carbon nitride particles, an enlarged section (1000–1400 cm^{-1}) of FTIR specra of NEt_4OH, bulk and colloidal CN, ^{13}C NMR spectrum of colloidal CN]. See DOI: 10.1039/b000000x/

1 A. Ciesielski and P. Samori, *Chem. Soc. Rev*. 2014, **43**, 381.
2 Y. Zhu, S. Murali, W. Cai, X. Li, J.W. Suk, J.R. Potts and R.S. Ruoff, *Adv. Mater.* 2010, **22**, 3906.
3 S. Park and R.S. Ruoff, *Nature Nanotechnol*. 2009, **4**, 217.
4 D.R. Dreyer, S. Park, C.W. Bielawski and R.S. Ruoff, *Chem. Soc. Rev*. 2010, **39**, 228.
5 C.N.R. Rao, H.S.S. Ramakrishna Matte and U. Maitra, *Angew. Chem. Int. Ed*. 2013, **52**, 2.
6 X. Lang, X. Chen and J. Zhao, *Chem. Soc. Rev*. 2014, **43**, 473.
7 J. Zhu, P. Xiao, H. Li and S.A.C. Carabineiro, *ACS Appl. Mater. Interfaces* 2014, **6**, 16449.
8 X. Wang, S. Blechert and M. Antonietti, *ACS Catal*. 2012, **2**, 1596.
9 F. Fresno, R. Portela, S. Suarez and J.M. Coronado, *J. Mater. Chem. A* 2014, **2**, 2863.
10 A. Thomas, A. Fischer, F. Goettmann, M. Antonietti, J.-O. Müller, R. Schlögl and J.M. Carlsson *J. Mater. Chem*. 2008, **18**, 4893.
11 Y. Zheng, J. Liu, J. Liang, M. Jaroniec and S.Z. Qiao, *Energy Environ. Sci*. 2012, **5**, 6717.
12 J. Hong, X. Xia, Y. Wang and R. Xu, *J. Mater. Chem*. 2012, **22**, 15006.
13 Y. Zhang, T. Mori, J. Ye and M. Antonietti, *J. Am. Chem. Soc*. 2010, **132**, 6294.
14 M. Shalom, S. Inal, C. Fettkenhauer, D. Neher and M. Antonietti, *J. Am. Chem. Soc*. 2013, **135**, 7118.
15 Y. Ishida, L. Chabanne, M. Antonietti and M. Shalom, *Langmuir* 2014, **30**, 447.
16 Y. Yin, J. Han, X. Zhang, Y. Zhang, J. Zhou, D. Muir, R. Sutarto, Z. Zhang, S. Liu and B. Song, *RSC Adv*. 2014, **4**, 32690.
17 X. Lu, K. Xu, P. Chen, K. Jia, S. Liu and C. Wu, *J. Mater. Chem. A* 2014, **2**, 18924.
18 H. Wang, Y. Su, X. Zhao, H. Yu, S. Chen, Y. Zhang and X. Quan, *Environ. Sci. Technol*. 2014, **48**, 11984.
19 H. Zhao, H. Yu, X. Quan, S. Chen, H. Zhao and H. Wang, *RSC Adv*. 2014, **4**, 624.
20 M. Liu, Z. Pei, S. Weng, Z. Fang, Z. Zheng, M. Huang and P. Liu, *Phys. Chem. Chem. Phys.* 2014, **16**, 21280.
21 J. Xu, L. Zhang, R. Shi and Y. Zhu, *J. Mater. Chem. A* 2013, **1**, 14766.
22 H. Zhao, H. Yu, X. Quan, S. Chen, Y. Zhang, H. Zhao and H. Wang *Appl. Catal. B* 2014, **152–153**, 46.
23 X. Zhang, H. Wang, H. Wang, Q. Zhang, J. Xie, Y. Tian, J. Wang and Y. Xie, *Adv. Mater*. 2014, **26**, 4438.
24 N. Cheng, J. Tian, Q. Liu, C. Ge, A.H. Qusti, A.M. Asiri, A.O. Al-Youbi, X. Sun, *ACS Appl. Mater. Interfaces* 2013, **5**, 6815.
25 X. Zhang, X. Xie, H. Wang, J. Zhang, B. Pan, Y. Xie, *J. Am. Chem. Soc*. 2013, **135**, 18.
26 M. Lu, Z. Pei, S. Weng, W. Feng, Z. Fang, Z. Zheng, M. Huang, P. Liu, *Phys. Chem. Chem. Phys*. 2014, **16**, 21280.
27 S. Yang, Y. Gong, J. Zhang, L. Zhan, L. Ma, Z. Fang, R. Vajtai, X. Wang, P.M. Ajayan, *Adv. Mater.* 2013, **25**, 2452.
28 J. Jiang, L. Ou-yang, L. Zhu, A. Zheng, J. Zou, X. Yi and H. Tang, *Carbon* 2014, **80**, 213.
29 X.-L. Zhang, C. Zheng, S.-S. Guo, J. Li, H.-H. Yang and G. Chen, *Anal. Chem*. 2014, **86**, 3426.

30 N. Cheng, P. Jiang, Q. Liu, J. Tian, A.M. Asiri and X. Sun *Analyst* 2014, **139**, 5065.
31 Y.V. Panasiuk, A.E. Raevskaya, A.L. Stroyuk and S.Ya. Kuchmiy, *Theoret. Experim. Chem.* 2014, **50**, 291.
32 E. Wirnhier, M.B. Mesch, J. Senker and W. Schnick, *Chem. Eur. J.* 2013, **19**, 2041.
33 J. Zhang, M. Zhang, C. Yang and X. Wang, *Adv. Mater*. 2014, **26**, 4121.
34 W.J. Jones and W.J. Orville-Thomas, *Trans. Faraday Soc*. 1959, **55**, 203.
35 L.J. Bellamy, *The Infra-red spectra of complex molecules*, London:Methuen & Co., New York: John Wiley & Sos, 1963.
36 S. Chu, C. Wang, J. Feng, Y. Wang and Z. Zou, *Inter. J. Hydrogen En*. 2014, **39**, 13519.
37 B. Jürgens, E. Irran, J. Senker, P. Kroll, H. Müller and W. Schnick, *J. Am. Chem. Soc*. 2003, **125**, 10288.
38 J.R. Holst and E.G. Gillan, *J. Am. Chem. Soc.* 2008, **130**, 7373.
39 S.J. Makowski, P. Köstler and W. Schnick, *Chem. Eur. J*. 2012, **18**, 3248.
40 J.A. Barltrop and J.D. Coyle, *Principles of Photochemistry*. John Wiley and Sons, Chichester, New York, Brisbane and Toronto, 1979, 214 p.